Pulsed gradient NMR study of anisotropic surfactant diffusion in the caesium perfluoro octanoate/D$_2$O system

Paul Ukleja[a]; G. Chidichimo[b]; P. Photinos[c]

[a] Department of Physics, Southeastern Massachusetts University, North Dartmouth, Massachusetts, U.S.A. [b] Department of Chemistry, University of Calabria, Arcavata, Italy [c] Department of Physics, South Oregon State College, Ashland, Oregon, U.S.A.

PLEASE SCROLL DOWN FOR ARTICLE

Pulsed gradient NMR study of anisotropic surfactant diffusion in the caesium perfluoro octanoate/D₂O system

by PAUL UKLEJA*

Department of Physics, Southeastern Massachusetts University,
North Dartmouth, Massachusetts 02747, U.S.A.

G. CHIDICHIMO

Department of Chemistry, University of Calabria, Arcavata, Italy

and P. PHOTINOS

Department of Physics, South Oregon State College, Ashland,
Oregon 97520, U.S.A.

We use pulsed field gradient ^{19}F NMR to measure the diffusion coefficients of surfactant molecules in the isotropic and lamellar phases of the caesium perfluoro octanoate (CsPFO)/D₂O system. An aligned lamellar sample is created by cooling through the nematic phase in the presence of a 1·4 T magnetic field. The director in the lamellar phase does not respond to ordinary field strengths, thus the aligned sample can be rotated clockwise or counterclockwise to place the director at a magic angle, where measurement of diffusion coefficients becomes possible. From a pair of so-obtained coefficients, we derive the principal values of the diffusion tensor corresponding to the directions parallel and perpendicular to the director ($D_\parallel$ and $D_\perp$). We found $D_\perp$ to be at least 20 times $D_\parallel$, a much larger anisotropy than is seen in electrical conductivity and water diffusion in similar systems. These results are compared to electrical conductivity, water and dye diffusion measurements.

1. Introduction

The phase diagram [1] of the micellar system caesium perfluoro octanoate (CsPFO)/D₂O shows many interesting features, and has received considerable attention in recent years. Of interest to the present work is the range of intermediate weight fraction, where the system shows a lamellar smectic, a micellar nematic and an isotropic phase. The micellar nematic phase occurs in a relatively narrow temperature and concentration range between the lamellar and the isotropic phase. The characteristic orientational order in the nematic phase results from the spontaneous alignment of the short axes of oblate or disc-shaped micelles. The preferential direction of this spontaneous alignment defines the optic axis or director of the phase. The lamellar smectic, or neat phase, bears many similarities to the smectic A phase exhibited by thermotropic liquid crystals. It is characterized by long range uniaxial orientational order and one-dimensional translational order. The latter occurs along the director of the phase. The isotropic phase results from the melting of the translational and/or orientational order.

* Author for correspondence.

A significant difference between the two ordered phases is that the director in the nematic phase readily aligns parallel to an externally applied magnetic field, whereas the director in the lamellar phase cannot be realigned by ordinary field values. Aligned lamellar phases are obtained by cooling from the nematic phase and simultaneously applying an aligning magnetic field. The so-obtained alignment of the lamellar smectic is rather good if the nematic to lamellar transition is second order. It was first observed by electric conductivity measurements on aligned samples [2] that the smectic planes of the lamellar phase are rather permeable to ions. In fact, the measurements did not show significant change in the conductivity along the director at the nematic to lamellar transition. These results were verified on several micellar systems. Qualitatively similar results were obtained for diffusion of water [3]. While these results leave little doubt as to the continuity for the aqueous region of the lamellar phase, in terms of the hydrophobic region the results can be interpreted equally well by assuming either continuous or discontinuous regions. In the first case we have essentially a perforated bilayer structure. In the second case the smectic planes consist of individual micelles. In the present work we report measurements of the diffusion coefficients of the hydrophobic tails. The measurements were taken on aligned samples of $CsPFO/D_2O$ in the lamellar phase, using the method of pulsed field gradient nuclear magnetic resonance of the ^{19}F nuclei of the CsPFO hydrophobic tails.

2. Experimental method

The method used is a variation of the pulsed gradient spin–echo NMR experiment in which the sample director, $\mathbf{n}$, is rotated to a magic angle $\pm\theta_m(\tan\theta_m = \sqrt{2})$ to the static field, where it becomes possible to produce a usable spin–echo. The field gradient is also directed along one of the magic angles so that diffusion is measured along an axis making an angle of either 0 or $2\theta_m$ with the director. This method was successfully applied in an earlier study of anisotropic diffusion in the smectic phases of potassium palmitate/D_2O, dipalmitoylphosphatidylcoholine (DPPC)/D_2O and $\bar{8}S5$ [4]. In the present work, the ^{19}F resonance is used so that the motion of the hydrophobic tails is studied. A recent review of pulsed gradient methods is given by Kärger *et al.* [5].

2.1. *Standard pulsed gradient method*

In the standard pulsed gradient spin echo experiment developed by Tanner and Stejskal [6] a matched pair of field gradient pulses of width δ is inserted into a $\pi/2$–τ–$\pi/2$ or stimulated echo–pulse sequence and attenuates the echo by a factor

$$R(\gamma g\delta, \Delta) = \exp[-D(\gamma g\delta)^2(\Delta - \delta/3)], \qquad (1)$$

where γ is the gyromagnetic ratio for the nuclei being observed, g is the applied field gradient, Δ is the time from the start of the first gradient pulse to the start of the second and D is the diffusion coefficient corresponding to translational motions in the direction of the gradient. The cross term between the applied and background field gradients is left out here as it was kept negligible.

The pulsed gradient experiment is sensitive to the mean-squared displacements of the molecules along the direction of the applied field gradient during the time between the gradient pulses. In samples exhibiting restricted diffusion, if the mean squared path is comparable to the spacing of restrictions then the values of D calculated using equation (1) depend on the parameter Δ. An alternate expression for the echo

attenuation that shows directly the dependence of the echo height on the molecular displacements is [7]

$$R(\gamma g \delta, \Delta) = \exp\left[-(\gamma g \delta)^2 \langle S(\Delta)^2 \rangle / 2\right], \tag{2}$$

where $S(\Delta)$ is the displacement of a molecule along the direction of the gradient during the diffusion time Δ. When diffusion obeys Fick's first law, a plot of $\ln(R)/(\gamma g \delta)^2$ versus Δ is a straight line through the origin with slope D. Restrictions with characteristic spacing d cause such a plot to curve downward in the region around $\Delta = d^2/2D$.

2.2. *Variation for smectic liquid crystals*

In most liquid crystal phases there are several complications that arise:

(1) Dipolar and other interactions broaden the resonance and drastically reduce echoes compared to an isotropic liquid.
(2) The anisotropy of the medium makes the diffusion depend on direction. In uniaxial samples, D is a function of the angle, θ, between the gradient and the director:

$$D(\theta) = D_{\parallel} \cos^2 \theta + D_{\perp} \sin^2 \theta, \tag{3}$$

where $D_{\parallel}$ and $D_{\perp}$, respectively, denote diffusion parallel and perpendicular to the director, **n**.
(3) The value of D may be extremely low, particularly for translations parallel to the director (perpendicular to the layers) in lamellar phases.

The broadening can be greatly reduced in a well-aligned smectic liquid crystalline sample by orienting the director along one of the magic angles [8, 9]. Doing this in our samples allowed production of a usable but small stimulated echo which could be detected up to several tenths of seconds after the initial pulse.

To address the second and third points, quadrupolar gradient coils were used which produced a large gradient, approximately 750 gauss/cm, directed along one of the magic angles. This allowed us to do the experiment in two orientations by rotating the sample either clockwise or counterclockwise to a magic angle (as shown in figure 1). In

SAMPLE IN CW POSITION   SAMPLE IN CCW POSITION

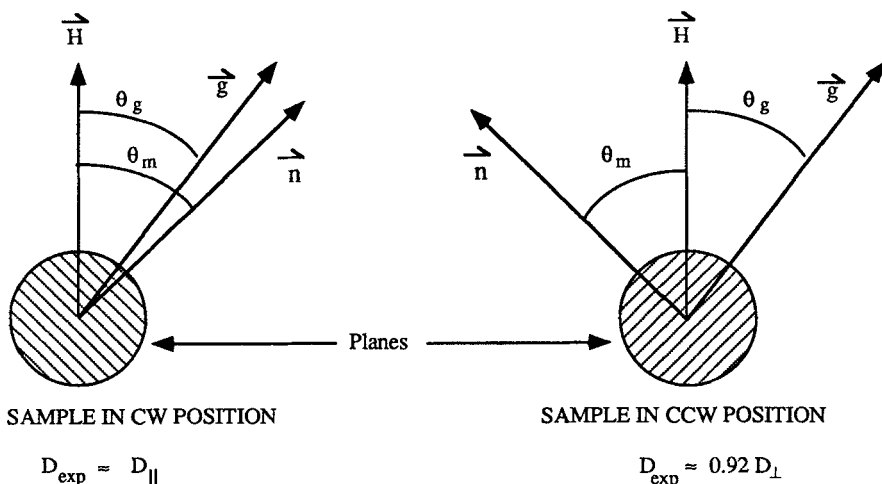$D_{exp} \approx D_{\parallel}$ $D_{exp} \approx 0.92\, D_{\perp}$

Figure 1. The sample in the CW and CCW positions, showing the orientations of the director, field gradient and static magnetic fields.

the clockwise position, the gradient and director were aligned to within a few degrees, giving the maximum sensitivity for determining $D_{\parallel}$.

The echo attenuations are measured in the two orientations and are used to calculate diffusion coefficients from equation (1). For the two measurements, θ takes on the values $\theta_g \pm \theta_m$, or approximately 0 and $2\theta_m$, respectively, where θ_g is the actual angle between the gradient and the static field as shown in figure 1 for both sample positions. From these measured coefficients the principal values of the diffusion tensor, $D_{\parallel}$ and $D_{\perp}$ are determined by means of equation (3).

3. Experimental details
3.1. *Sample preparation*

Caesium perfluoro octanoate was prepared by neutralizing pentadecafluoro octanoic (98 per cent purity, Aldrich) with CsOH (99·9 per cent purity, Aldrich). The salt was filtered and recrystalized three times from cold ethanol. For the measurements we used a sample consisting of 50 per cent by weight mixture of CsPFO in D_2O (99·8 per cent purity, Aldrich). The sample was mixed by mechanical stirring for several days, and was stored at 50°C before use. At room temperature the sample is in the lamellar phase; it becomes nematic at 42°C and isotropic at 48°C. According to the phase diagram of Boden *et al.* [1] the lamellar to nematic transition is second order at this composition.

The sample was placed in a thin-walled, flat-bottomed, 7·5 mm o.d. NMR tube. A removable plug was placed 2–3 mm above the surface of the sample to minimize the water loss to condensation in empty parts of the tube and to allow addition of water if needed. The composition changed 2–3 per cent during the measurements, as indicated by the drift in transition temperatures. The values obtained for $D_{\perp}$ in the smectic phase (near room temperature) did not show any strong correlation with the sample age. The measurements in the isotropic phase were taken at 52°C and 62°C, after the measurements done in the smectic phase, and at these temperatures the sample composition changed more rapidly. This change in composition was reflected as a decrease with time in the measured values of D in the isotropic phase. Time and apparatus constraints did not allow a repetition of the experiments.

3.2. *Apparatus*

The experiment was performed at the Liquid Crystal Institute, Kent, Ohio, using a JEOL JNM-PS-100 magnet and parts of a Bruker model B-KR322S spectrometer with the addition of a Nicolet 1180E data-acquisition system, and home-made programmable pulse generator and quadrature phase-sensitive detector. The measurements were performed at a fluorine frequency close to 60 MHz. Temperature was controlled using an Omega CN-2010 controller and a heater coil wound on the NMR probe. A platinum temperature sensor was placed in the copper block close to the sample.

The temperature-regulated NMR probe had quadrupolar field gradient coils constructed as described by Zupančič and Pirš [10]. The gradient coils were rotated to set the gradient as parallel as possible to the director in the CW position and make the measurements as sensitive as possible to the expected low values of $D_{\parallel}$. The actual angle between the gradient and the Z axis, θ_g, was determined to be $51 \pm 1°$ by measuring the diffusion coefficient of HOD (partially deuterated water) in an aligned sample of DPPC and water with the director at several angles near θ_g [4, p. 428]. The magic angle could be located accurately due to the sharp increase in T_2 of the lipid. The value of θ_g was verified to an accuracy of 2° by observing the FID of a water sample in a rectangular

cross-sectioned tube when a small current was passed through the gradient coils. Using this value of θ_g in equations (3) yields the following relations:

$$D_\perp = 1 \cdot 080 D_{ccw} - 0 \cdot 080 D_{cw}, \tag{4 a}$$

$$D_{\parallel} = 1 \cdot 0046 D_{cw} - 0 \cdot 0046 D_{ccw}, \tag{4 b}$$

where D_{cw} and D_{ccw} correspond to the values obtained in the clockwise and counter-clockwise positions, respectively. Typically, D_{cw} was less than $D_{ccw}/20$, so that the contribution of D_{cw} to $D_\perp$ in equation (4 a) could be neglected and $D_\perp$ be determined accurately from a measurement of D_{ccw}. The corresponding 'cross term' in equation (4 b) typically contributed about 10 per cent to the value of $D_{\parallel}$. The uncertainties introduced through the uncertainty in θ_g are negligible here.

Calibration of the areas of gradient pulses ($g\delta$) was performed by observing echo attenuations using water at 25°C and 45°C with a range of gradient pulse widths and separations and comparing to published values [11]. The ratio between values measured at the two temperatures agreed with the published values to about 2 per cent. For widths greater than 40 μs, the expression $(7 \cdot 26 \, T/m) \, (\delta\text{-}9 \, \mu s)$ was used for δg in equations (1) and (2) to take into account the rise and fall times of the gradient pulses.

3.3. *Sequence*

In order to be able to determine the values of D_{cw}, which were around $2 \times 10^{-12} \, m^2/s$, it was necessary to use the stimulated echo [12]. The time between sequences was 2 s, to avoid heating and to allow the magnetization to relax. The pulse sequence is synchronized so each gradient pulse starts at the same part of the 60 Hz cycle, avoiding some of the worst noise problems. The separation between the first two r.f. pulses had to be kept less than around 1·5 ms because of the rapid decrease in echo with this time. This resulted in a maximum value of 600 μs for δ, in order to avoid distorting the echo or interfering with the r.f. pulse.

The background field gradient, g_0, was kept less than 0·0035 T/m in these experiments, to remove the effect of the cross-term (bilinear in g and g_0). To ensure that the cross-term could be neglected, the experiments were usually repeated with the gradient coils electrically reversed, changing the sign of the bilinear term, but not the g^2 or g_0^2 terms. No significant differences in the echo attenuations were observed when this was done. The separation of the gradient pulses was varied between 10 and 200 ms for the D_{ccw} measurements and 200 and 400 ms for the D_{cw} measurements. The width of the second of each pair of gradient pulses could be varied by small amounts to balance the pulses and produce the maximum echo in the correct location.

The gradient pulse widths were alternated between 10 μs and the chosen value of δ. The 10 μs pulses were used to destroy (in a recoverable manner) the transverse magnetization before the second r.f. pulse, but were too small to cause any diffusion-related attenuation. The alternate echoes (with and 'without' gradient pulses) were acquired and averaged separately. The values for D, unless otherwise noted below, were obtained via equation (1) from observations of the ratio R (typically averaged 10–25 times for a given set of values of δ, Δ and the width adjustment on the second gradient pulse), of the two so-obtained echo heights.

4. Results
4.1. *Temperature dependence*

Values determined for $D_{\parallel}$ and $D_\perp$ in the smectic phase and for D_{is} in the isotropic phase are shown in figure 2. In the smectic phase the points for D_{is} correspond to an
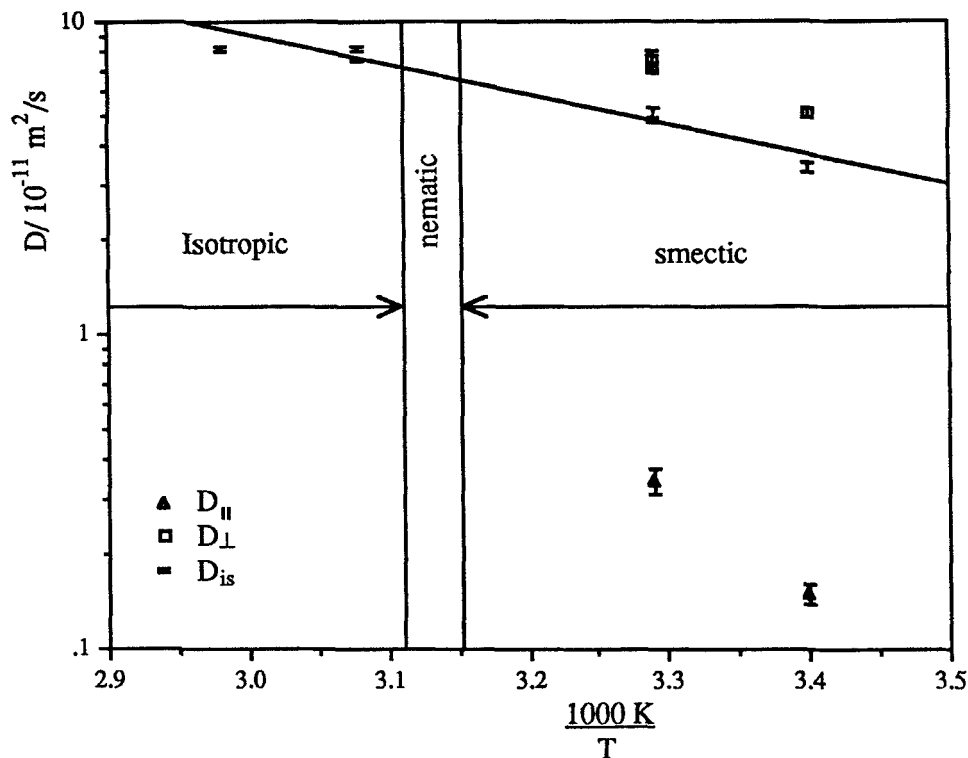
P. Ukleja *et al.*

Figure 2. $D_{\parallel}$, $D_{\perp}$ and D_{is} versus $1000\,\mathrm{K}/T$ for the surfactant in the smectic and isotropic phases of the CsPFO/water system. Errors shown are statistical uncertainties only. The line shown is the weighted least squares fit of $\ln(D_{is})$ to the line $m(1/T)+b$.

isotropic average, $(2D_{\perp}+D_{\parallel})/3$. Each point represents an average of the values obtained using equation (1) and repeated measurements of the echo heights with different values of δ and Δ. The error bars are statistical only, the standard errors associated with averaging these individual D values. The line shown in the figure is a weighted least squares fit of the D_{is} values to the equation $\ln(D)=a-E_a/RT$, with $E_a=4\,\mathrm{kcal/mole}$.

4.2. *Restricted diffusion*

There was some suggestion of a dependence of $D_{\perp}$ on the diffusion time in the experiment, which might be taken to be evidence that translational diffusion is restricted on this time and distance scale [6]. This could also arise from instrumental problems such as a shock transferred from the gradient coils to the sample, or echo distortion by residual gradients, or could arise from internal gradients. In polymer melts, for instance, Bachus and Kimmich [13] found that inhomogeneities in the medium create internal field gradients which cannot always be neglected in this kind of experiment.

To investigate the possibility of restricted diffusion, Δ was varied between 10 ms and 200 ms for the determinations of $D_{\perp}$ at 21°C and 31°C. We have plotted $-2\ln(R)/(\gamma g\delta)^2$ versus Δ for the 31°C data in figure 3 so that the vertical axis corresponds to mean square displacements along the direction of the gradient, in accordance with equation
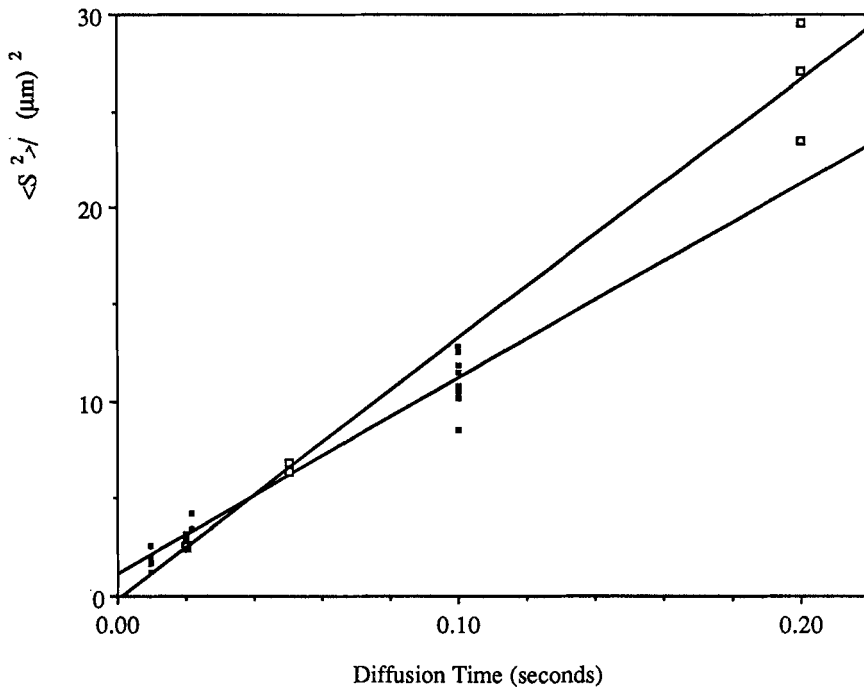
Figure 3. Mean square displacement, $\langle S^2 \rangle$, along the direction of the gradient versus diffusion time, Δ at 31°C. The values of $\langle S^2 \rangle$ are calculated from the echo attenuations using equation (2). The solid squares represent data taken the first day, while the open squares represent data taken after several days at 31°C. The lines represent fits of each day's data to the form $\ln(R) = a - b\Delta$ and correspond to values for D of 5·0 and 6·7 × 10^{-11} m²/s for the solid and open squares, respectively.

(2). Each point on this graph represents a series of 4–25 repetitions measuring echo attenuation for a particular setting of pulse width and separation. The vertical scatter of points on the figure was uncorrelated with pulse width, but was because of, for instance, instrumental problems such as instabilities in the magnetic field. Most instrumental mishaps reduce the echo and cause points to lie high on this kind of plot and become more likely when longer values of δ or Δ are used. On the other hand, restrictions in diffusion show as downward bending at the point when the rms displacements are on the order of the spacings of restrictions.

The data taken the first day at 31°C (solid squares) shows evidence of bending at diffusion times of 0·1 s as did the data taken slightly earlier at 21°C, although, given the scatter of the points, it may not be significant. This corresponds to restrictions spaced about 3–4 μm apart. Most of the preliminary experiments showed a similar behaviour, that is, such plots always fit to straight lines with positive (but not highly significant) intercepts. The open squares in the figure represent a repetition of the experiment several days later, during which time the sample remained at the magic angle at 31°C. This repetition shows no evidence of restriction at 0·2 s (5 μm) which could be because of annealing of defects. Taking all the points as a whole, one can fit a reasonable-looking straight line to all the data, essentially what was done in the value reported in figure 2. The accuracy of these measurements is not great enough to make any strong

claims of having observed restrictions and annealing of restrictions and we would like to pursue these matters in future experiments.

5. Conclusions

We measured the anisotropic diffusion coefficients of the surfactant tails in the isotropic and lamellar smectic phases. Measurements in similar micellar systems have been presented for the diffusion of water [3], for the diffusion of oil soluble dyes [14] and for the diffusion of water, lithium ions and surfactant [15]. The diffusion of water is more rapid, and the corresponding D values are about two orders of magnitude higher than what we measured for the surfactant molecules. The diffusion of the oil soluble dye (Oil Blue A, DuPont) was measured on the decylammonium chloride system and only for the $D_\perp$ component. The measured value is in very good agreement with our $D_\perp$ values. The value of $D_\perp$ for the surfactant in lithium PFO was over an order of magnitude smaller than our values.

A measure of the anisotropy of the structure of the aqueous and the hydrophobic regions in the lamellar phase is given by the reduced anisotropy: $\alpha = (D_\perp - D_\parallel)/\langle D \rangle$ where the average value $\langle D \rangle = (D_\parallel + 2D_\perp)/3$. The water diffusion measurements of Chidichimo *et al.* [3] give $\alpha = 0.35$, which is comparable to the anisotropy of the ionic conductance for the lamellar phase [16]. The values for α obtained by Tiddy [15] were 0.25–0.4 for water and 0.06 for Li^+. On the other hand, we observe $\alpha = 1.4$ for the diffusion of CsPFO. This is a rather high value, considering that the maximum possible value for α is 1.5. The diffusion anisotropy of CsPFO measured here is very close to the values measured on DPPC/water mixtures [4], which form rather continuous lamellae, have highly anisotropic water diffusion and do not show micellar nematic phases. The self-diffusion measurements in thermotropic smectics show a wide range of anisotropies. The values reported for the thermotropics [4, 17] are generally smaller than our values for the CsPFO lamellar smectic, and the DPPC bilayers [4].

The different values for the diffusion anisotropy of the water and CsPFO molecules reflect the difference between the structure of the aqueous region and the hydrophobic region of the lamellar phase. The aqueous region occupies about 73 per cent of the volume and is rather continuous, in comparison to the hydrophobic region. The diffusion of water is mathematically analogous to the ionic conductance. For the latter, calculations based on specific models have been presented [18] for both perforated lamellae and for discs. The calculation for the perforated lamellae [19] can be extended to interpret the diffusion anisotropy of the CsPFO ions. By extrapolation of the values of Photinos and Saupe [16] we find that for volume fraction of about 70 per cent the measured anisotropies correspond to defect values less than 5 per cent. The nature of the defects in the lamellar phases has been discussed in detail by Helfrich [20]. The TEM micrographs of Sammon *et al.* [21] on the decylammonium chloride system show that a large number of screw dislocations indeed occur in the lamellar phase. In a lamellar smectic consisting of stacked bilayers, these dislocations would be the primary cause for the finite $D_\parallel$ values. More detailed measurements at different concentrations, as well as numerical calculations of the diffusion anisotropy from model structures are presently underway.

References

[1] BODEN, N., CORNE, S., and JOLLEY, K., 1987, *J. phys. Chem.*, **91**, 4092.
[2] PHOTINOS, P., YU, L. J., and SAUPE, A., 1981, *Molec. Crystals liq. Crystals*, **67**, 277.
[3] CHIDICHIMO, G., COPPOLA, L., LA MESA, G., RANIERI, G. A., and SAUPE, A., 1988, *Chem. Phys. Lett.*, **145**, 85.
[4] UKLEJA, P., and DOANE, J. W., 1980, *Ordering in Two Dimensions*, edited by S. K. Sinha (North-Holland), pp. 427–429.
[5] KÄRGER, J., PFEIFER, H., and HEINK, W., 1988, *Adv. magn. Reson.*, **12**, 1.
[6] TANNER, J. E., and STEKSKAL, E. O., 1968, *J. chem. Phys.*, **49**, 1768.
[7] KÄRGER, J., PFEIFER, H., and VOJTA, G., 1988, *Phys. Rev. A*, **37**, 4514.
[8] DOANE, J. W., and PARKER, R. S., 1973, *XVIIIth Cong. Ampère*, p. 410.
[9] ROEDER, S. B. W., and BURNELL, E. E., 1976, *J. chem. Phys.*, **64**, 1848.
[10] ZUPANČIČ, I., and PIRŠ, J., 1976, *J. Phys. E*, **9**, 79.
[11] LONGSWORTH, L. G., 1960, *J. phys. Chem.*, **64**, 1914.
[12] TANNER, J. E., 1970, *J. chem. Phys.*, **52**, 2523.
[13] BACHUS, R., and KIMMICH, R., 1983, *Polymer*, **24**, 964.
[14] GAULT, J. D., KAVANAGH, E., RODRIGUES, L. A., and GALLARDO, H., 1986, *J, phys. Chem.*, **90**, 1860.
[15] TIDDY, G. J. T., 1977, *J. chem. Soc. Faraday Trans I*, **73**, 1731. Note that the definitions of $D_\perp$ and $D_\parallel$ are reversed from our usage.
[16] PHOTINOS, P. J., and SAUPE, ALFRED., 1986, *J. chem. Phys.*, **85**, 7647.
[17] KRUGER, G. J., 1982, *Phys. Rep.* **82**, 229.
[18] PHOTINOS, P., and SAUPE, A., 1986, *J. chem. Phys.*, **84**, 517. Note that this work uses a different definition for the anisotropy.
[19] The results for the discs cannot be directly applied to the diffusion of the CsPFO ions.
[20] HELFRICH, W., 198X, *Les Houches Session XXXV* (North-Holland), Chap. 11.
[21] SAMMON, M. J., ZASADZINSKI, J. A. N., and KUZMA, M. R., 1986, *Phys. Rev. Lett.*, **57**, 2834.